Journal of Theoretical Biology 258 (2009) 403–417

Contents lists available at ScienceDirect

Journal of Theoretical Biology

journal homepage: www.elsevier.com/locate/yjtbi

Spatial spreading of West Nile Virus described by traveling waves ☆

Norberto Aníbal Maidana *,[1], Hyun Mo Yang [2]

UNICAMP – IMECC/DMA, Caixa Postal 6065, CEP: 13083-859, Campinas, SP, Brazil

ARTICLE INFO

Article history:
Received 1 February 2008
Received in revised form
27 November 2008
Accepted 2 December 2008
Available online 6 January 2009

Keywords:
West Nile Virus
Reaction–diffusion equation
Traveling waves
Wave speed
Sensitivity analysis

ABSTRACT

In this work, we propose a spatial model to analyze the West Nile Virus propagation across the USA, from east to west. West Nile Virus is an arthropod-borne flavivirus that appeared for the first time in New York City in the summer of 1999 and then spread prolifically among birds. Mammals, such as humans and horses, do not develop sufficiently high bloodstream titers to play a significant role in the transmission, which is the reason to consider the mosquito–bird cycle. The model aims to study this propagation based on a system of partial differential reaction–diffusion equations taking the mosquito and the avian populations into account. Diffusion and advection movements are allowed for both populations, being greater in the avian than in the mosquito population. The traveling wave solutions of the model are studied to determine the speed of disease dissemination. This wave speed is obtained as a function of the model's parameters, in order to assess the control strategies. The propagation of West Nile Virus from New York City to California state is established as a consequence of the diffusion and advection movements of birds. Mosquito movements do not play an important role in the disease dissemination, while bird advection becomes an important factor for lower mosquito biting rates.

1. Introduction

West Nile Virus (WNV) is an arthropod-borne flavivirus. The primary vectors of WNV are *Culex* spp. mosquitoes, although the virus has been isolated from at least 29 more species of 10 genera (Campbell et al., 2002). When an infected mosquito bites a bird, the virus is transmitted. A mosquito is infected when it bites an infected bird. Also, the virus can be vertically transmitted from a mosquito to its offspring.

The intensity of transmission to human depends on the abundance and feeding patterns of infected mosquitoes, on the local ecology and behaviors that influence human exposure to mosquitoes (Hayes et al., 2005). Mammals, such as humans and horses, do not develop sufficiently high bloodstream titers to play a significant role in the transmission (DeBiasi and Tyler, 2006; Hayes, 1989), and this is a reason to consider the mosquito–bird cycle.

One major feature of WNV spatial dissemination is the high velocity of geographic invasion and colonization. This is due to the long distance flight of birds, and to the ubiquitous presence of mosquitoes. For instance, WNV was introduced in New York City in 1999, and then propagated across the USA. After five years, WNV was detected among birds in California, western USA.

Mathematical models which did not encompass spatial dynamics were developed by Kenkre et al. (2005), Wonham et al. (2004), Cruz-Pacheco et al. (2005) and Bowman et al. (2005). Those models considered different aspects of the WNV disease and determined threshold conditions with respect to control strategies. Kenkre et al. (2005) studied the periodicity of the infection considering vertical transmission, increase in mortality due to infection and time scale disparity. Wonham et al. (2004) considered the whole mosquito's life cycle. Cruz-Pacheco et al. (2005) took into account experimental data from the literature to estimate threshold values regarding several species of birds. The effects of vertical transmission on the disease dynamics were also studied, and different recovery rates were considered for different species of birds. In Bowman et al. (2005), they added the human population in order to assess preventive strategies.

With respect to spatial models, Lewis et al. (2006) considered in their model the corresponding spatially homogeneous modeling proposed by Wonham et al. (2004). They studied the propagation of WNV using traveling wave solutions for a simplified model, which did not consider vertical transmission, as well as the mortality rate induced by WNV disease and the recovered avian subpopulation. Aiming to determine the biological invasion of WNV from the east to the west coast of the USA, we develop a spatio-temporal model to study this propagation as a consequence of the zoonotic characteristic of WNV.

☆ Grant from FAPESP (Projeto Temático).
* Corresponding author. Tel.: +55 19 32874223.
E-mail addresses: nmaidana@ime.unicamp.br (N.A. Maidana), hyunyang@ime.unicamp.br (H.M. Yang).
[1] Fellowship from FAPESP (Postdoctoral fellowship).
[2] Fellowship from CNPq.

0022-5193/$ - see front matter © 2009 Elsevier Ltd. All rights reserved.
doi:10.1016/j.jtbi.2008.12.032

Since Fisher (1937) proposed a model to study the propagation of an advantageous gene in terms of reaction–diffusion equation, a large number of studies have been made about the biological invasion process using that kind of reaction–diffusion equation. The first work to describe the spatial propagation of a disease was developed by Källen et al. (1985). In that work, a directly transmitted infectious disease model was studied to describe the propagation of rabies among foxes. A simple model developed in terms of the reaction–diffusion equations was studied to determine the first front wave of propagation. More realistic models were studied after that work in order to determine the cyclic epidemic of the front wave of rabies considering the growth of susceptible fox population and immunity (Murray et al., 1986; Murray and Seward, 1992). For indirectly transmitted diseases (by vectors) recent works were developed by Lewis et al. (2006) to study the spatial propagation of WNV, and by Maidana and Ferreira (2008) to study the propagation of the hip hop disease in capybaras.

Our model concerning the spatial dynamics of WNV allows the diffusion to both avian and mosquito populations, taking into account the fact that the diffusion coefficient in the avian population is greater than the diffusion in the mosquito population. From the model we seek the traveling waves connecting two steady states, which are the disease-free and the endemic equilibria, from which we determine the wave speed of propagation of WNV disease. We also study the sensitivity of the wave speed with respect to the variations in the essential parameters of the model. In recent experiments, Komar et al. (2003) studied 25 species of birds exposed to WNV by *Culex tritaniorhynchus* bites in order to evaluate the transmission dynamics. We apply their estimations to our model considering the species that are more competent for WNV transmission, determining the role of different species of birds in disease propagation.

At first, we consider a biting rate of 0.5, that is, once every two days (Cruz-Pacheco et al., 2005). Okubo (1998) estimated that the diffusion coefficient of birds ranged between 0 and 14 km^2/day. Choosing a coefficient for avian diffusion equal to 6 km^2/day, without advection and considering parameters for two species of birds—blue jay and common grackle—we obtain approximately 3 km/day for the velocity of disease propagation, which is consistent with that observed in field data. If we consider a biting rate of 0.3, as did Lewis et al. (2006), the wave speed decreases to 1.98 km/day. An advection velocity of 1.6−2.37 km/day is needed to match with the speed range of 3−3.5 km/day observed in field data. If we consider $b = 0.1$ (Wonham et al., 2004), a higher value for advection is needed to be comparable with the observed data.

The paper is structured as follows. In Section 2, a WNV spatial propagation model is presented, together with the analysis of the corresponding spatial homogeneous model. In Section 3, the minimum speed of the traveling wave is determined. The sensitivity analysis of the wave speed is assessed in Section 4, and this is used to describe the geographic spread in Section 5. In Section 6, we present numerical simulation to determine the wave speed graphically and conclusion is given in Section 7.

2. Model for WNV disease

We present a spatial model for WNV propagation and the analysis of the corresponding spatially homogeneous model for WNV disease.

2.1. Model for the spatial WNV propagation dynamics

WNV disease first appeared in North America in the summer of 1999, with the simultaneous occurrence of an unusual number of deaths of exotic birds and crows in New York City (DeBiasi and Tyler, 2006). During the next five years WNV propagated across the USA. We propose a model to study this propagation across the USA.

The spatially homogeneous model proposed in Cruz-Pacheco et al. (2005) includes cross-infection between the avian and the vector populations, whose densities are denoted by $\overline{N}_a(t)$ and $\overline{N}_v(t)$, respectively. The avian population was divided into susceptible, infective and recovered subpopulations, $\overline{S}_a$, $\overline{I}_a$ and $\overline{R}_a$, respectively, while the vector population was divided into susceptible and infected subpopulations, $\overline{S}_v$ and $\overline{I}_v$. The total populations are $\overline{N}_a(t) = \overline{S}_a(t) + \overline{I}_a(t) + \overline{R}_a(t)$ and $\overline{N}_v(t) = \overline{S}_v(t) + \overline{I}_v(t)$.

The mosquito population is regarded as constant, assuming that the birth and death rates are equal to $\overline{\mu}_v$. For the avian population, however, the total population density is allowed to vary, where Λ_a is the constant recruitment birth rate, and the death rate is $\overline{\mu}_a$. The differential equation for the avian population irrespective of WNV infection is then

$$\frac{d\overline{N}_a}{dt} = \Lambda_a - \overline{\mu}_a \overline{N}_a.$$

The biting rate b of mosquitoes is defined as the average number of bites per mosquito per day. $\overline{\beta}_a$ and $\overline{\beta}_v$ are the transmission probabilities from vector to bird and from bird to vector, respectively. Hence, the infection rates per susceptible birds and susceptible vectors are given by

$$b\overline{\beta}_a \frac{\overline{N}_v}{\overline{N}_a}\frac{\overline{I}_v}{\overline{N}_v} = b\frac{\overline{\beta}_a}{\overline{N}_a}\overline{I}_v \quad \text{and} \quad b\overline{\beta}_v \frac{\overline{I}_a}{\overline{N}_a}.$$

The birds are recovered at rate $\overline{\gamma}_a$. The specific death rate associated with WNV in the avian population is $\overline{\alpha}_a$, with $\overline{\alpha}_a \leqslant \overline{\gamma}_a$, according to Cruz-Pacheco et al. (2005). Another assumption is that mosquitoes can transmit WNV vertically. The fraction of progeny of mosquitoes that are infectious is denoted by p, with $0 \leqslant p \leqslant 1$.

From now on, we consider the spatio-temporal dependence on the populations, e.g. $N_a(x,t)$ and $N_v(x,t)$, and their respective subpopulations. The diffusion among birds is denoted by D_a, and D_v is designed for the diffusion of the mosquito population. We are not taking into account long migratory movements of birds, which occur in the north–south direction (Rappole et al., 2000). The mosquitoes are considered as a sessile population, then $D_v \ll D_a$. For instance, the mean dispersal distance for *Aedes aegypti* was ranged from 28 to 199 m, according to Harrington et al. (2005).

However, small advection movements are allowed for both populations in order to assess the stopover of the migratory birds during their long journey (Erni et al., 2002). The advection coefficients are denoted by $\overline{v}_a$ and $\overline{v}_v$ for avian and mosquito populations, respectively, with $\overline{v}_v \ll \overline{v}_a$. Our main goal in retaining the small advection movements is to analyze its relative importance in the overall WNV dissemination. The same diffusion and advection coefficients are considered in the infected (avian and mosquito) subpopulations considering that WNV disease does not affect their movements. The notation of the parameters is summarized in Table 1.

Based on the above assumptions and definitions of the parameters, the spatial model is the following:

$$\frac{\partial \overline{S}_a}{\partial t} = D_a \frac{\partial^2 \overline{S}_a}{\partial x^2} - \overline{v}_a \frac{\partial \overline{S}_a}{\partial x} + \Lambda_a - \frac{b\overline{\beta}_a}{\overline{N}_a}\overline{I}_v \overline{S}_a - \overline{\mu}_a \overline{S}_a, \tag{1}$$

$$\frac{\partial \overline{I}_a}{\partial t} = D_a \frac{\partial^2 \overline{I}_a}{\partial x^2} - \overline{v}_a \frac{\partial \overline{I}_a}{\partial x} + \frac{b\overline{\beta}_a}{\overline{N}_a}\overline{I}_v \overline{S}_a - (\overline{\gamma}_a + \overline{\mu}_a + \overline{\alpha}_a)\overline{I}_a, \tag{2}$$

Table 1
Summary of common notations.

	Vector	Reservoir
State variables		
Susceptible	$\overline{S}_v$	$\overline{S}_a$
Infectious	$\overline{I}_v$	$\overline{I}_a$
Recovered	–	$\overline{R}_a$
Total	$\overline{N}_v$	$\overline{N}_a$
Parameters		
Birth	$\overline{\mu}_v$	Λ_a
Death (natural)	$\overline{\mu}_v$	$\overline{\mu}_a$
Death (due to disease)	–	$\overline{\alpha}_a$
Recovery (from disease)	–	$\overline{\gamma}_a$
Virus transmission (to)	$\overline{\beta}_v$	$\overline{\beta}_a$
Vertical transmission	p	–
Diffusion	D_v	D_a
Advection	$\overline{v}_v$	$\overline{v}_a$

$$\frac{\partial \overline{R}_a}{\partial t} = D_a \frac{\partial^2 \overline{R}_a}{\partial x^2} - \overline{v}_a \frac{\partial \overline{R}_a}{\partial x} + \overline{\gamma}_a \overline{I}_a - \overline{\mu}_a \overline{R}_a, \tag{3}$$

$$\frac{\partial \overline{S}_v}{\partial t} = D_v \frac{\partial^2 \overline{S}_v}{\partial x^2} - \overline{v}_v \frac{\partial \overline{S}_v}{\partial x} + \overline{\mu}_v \overline{S}_v + (1-p)\overline{\mu}_v \overline{I}_v - \frac{b\overline{\beta}_v}{\overline{N}_a} \overline{I}_a \overline{S}_v - \overline{\mu}_v \overline{S}_v, \tag{4}$$

$$\frac{\partial \overline{I}_v}{\partial t} = D_v \frac{\partial^2 \overline{I}_v}{\partial x^2} - \overline{v}_v \frac{\partial \overline{I}_v}{\partial x} + p\overline{\mu}_v \overline{I}_v + \frac{b\overline{\beta}_v}{\overline{N}_a} \overline{I}_a \overline{S}_v - \overline{\mu}_v \overline{I}_v. \tag{5}$$

Let us introduce the non-dimensional parameters to system (1)–(5). The time is scaled with respect to bm, where b is the biting rate of mosquitoes, and $m = \overline{N}_v/(\Lambda_a/\overline{\mu}_a)$, the ratio of the vector population to the disease-free equilibrium bird population. The spatial variable is scaled considering the bird diffusion coefficient, according to $\sqrt{D_a/bm}$. The remaining non-dimensional parameters are

$$S_a = \frac{\overline{S}_a}{\Lambda_a/\overline{\mu}_a}, \quad I_a = \frac{\overline{I}_a}{\Lambda_a/\overline{\mu}_a}, \quad R_a = \frac{\overline{R}_a}{\Lambda_a/\overline{\mu}_a},$$

$$N_a = \frac{\overline{N}_a}{\Lambda_a/\overline{\mu}_a}, \quad S_v = \frac{\overline{S}_v}{\overline{N}_v}, \quad I_v = \frac{\overline{I}_v}{\overline{N}_v},$$

$$D = \frac{D_v}{D_a}, \quad v_a = \frac{\overline{v}_a}{bm}\left(\frac{bm}{D_a}\right)^{1/2}, \quad v_v = \frac{\overline{v}_v}{bm}\left(\frac{bm}{D_a}\right)^{1/2},$$

$$\mu_a = \frac{\overline{\mu}_a}{bm}, \quad \gamma_a = \frac{\overline{\gamma}_a}{bm}, \quad \alpha_a = \frac{\overline{\alpha}_a}{bm},$$

$$\mu_v = \frac{\overline{\mu}_v}{bm}, \quad \beta_a = \overline{\beta}_a, \quad \beta_v = \frac{\overline{\beta}_v}{m}.$$

Let us use $N_a = S_a + I_a + R_a$ and $S_v + I_v = 1$ to simplify system (1)–(5), then the corresponding non-dimensional model is

$$\frac{\partial S_a}{\partial t} = \frac{\partial^2 S_a}{\partial x^2} - v_a \frac{\partial S_a}{\partial x} + \mu_a - \frac{\beta_a}{N_a} I_v S_a - \mu_a S_a, \tag{6}$$

$$\frac{\partial I_a}{\partial t} = \frac{\partial^2 I_a}{\partial x^2} - v_a \frac{\partial I_a}{\partial x} + \frac{\beta_a}{N_a} I_v S_a - (\gamma_a + \mu_a + \alpha_a) I_a, \tag{7}$$

$$\frac{\partial I_v}{\partial t} = D\frac{\partial^2 I_v}{\partial x^2} - v_v \frac{\partial I_v}{\partial x} + \frac{\beta_v}{N_a} I_a (1 - I_v) - (1-p)\mu_v I_v, \tag{8}$$

$$\frac{\partial N_a}{\partial t} = \frac{\partial^2 N_a}{\partial x^2} - v_a \frac{\partial N_a}{\partial x} + \mu_a - \mu_a N_a - \alpha_a I_a. \tag{9}$$

2.2. Model for the spatially homogeneous WNV dynamics

The spatially homogeneous model corresponding to system (6)–(9) is the following:

$$\frac{dS_a}{dt} = \mu_a - \frac{\beta_a}{N_a} I_v S_a - \mu_a S_a, \tag{10}$$

$$\frac{dI_a}{dt} = \frac{\beta_a}{N_a} I_v S_a - (\gamma_a + \mu_a + \alpha_a) I_a, \tag{11}$$

$$\frac{dI_v}{dt} = \frac{\beta_v}{N_a} I_a (1 - I_v) - (1-p)\mu_v I_v, \tag{12}$$

$$\frac{dN_a}{dt} = \mu_a - \mu_a N_a - \alpha_a I_a. \tag{13}$$

The system of equations (10)–(13) has two steady states. The first one is the disease-free equilibrium point given by

$$P_0 = (1, 0, 0, 1).$$

For $p < 1$, the second one is the endemic state:

$$P_1 = (S_a^*, I_a^*, I_v^*, N_a^*),$$

where S_a^*, I_v^* and N_a^* are given by

$$S_a^* = \frac{\mu_a - (\gamma_a + \mu_a + \alpha_a) I_a^*}{\mu_a}, \quad I_v^* = \frac{\mu_a \beta_v I_a^*}{[\beta_v \mu_a - \alpha_a (1-p)\mu_v] I_a^* + (1-p)\mu_v \mu_a},$$

$$N_a^* = \frac{\mu_a - \alpha_a I_a^*}{\mu_a},$$

where I_a^* is the unique positive root in $(0, \mu_a/\mu_a + \alpha_a + \gamma_a)$ of the second degree polynomial

$$r(I_a) = eI_a^2 + fI_a + g$$

with the coefficients

$$e = [\beta_v \mu_a - \alpha_a (1-p)\mu_v]\frac{\alpha_a}{\mu_a},$$

$$f = 2\alpha_a (1-p)\mu_v - \beta_v \mu_a - (1-p)\mu_v(\gamma_a + \mu_a + \alpha_a)R_0,$$

$$g = \mu_a (1-p)\mu_v (R_0 - 1).$$

A positive solution always exists for $R_0 > 1$ and $p < 1$, where

$$R_0 = \frac{\beta_a \beta_v}{(1-p)\mu_v(\gamma_a + \mu_a + \alpha_a)} \tag{14}$$

is the basic reproductive number. In Appendix A, we show that the disease-free equilibrium point P_0 is locally asymptotically stable for $R_0 < 1$, otherwise the endemic state P_1 is stable. Hence, forward bifurcation occurs at $R_0 = 1$.

In the original parameters, the threshold value R_0 is

$$R_0 = \frac{mb^2 \overline{\beta}_a \overline{\beta}_v}{(1-p)\overline{\mu}_v(\overline{\gamma}_a + \overline{\mu}_a + \overline{\alpha}_a)} = \frac{mb\overline{\beta}_v}{(\overline{\gamma}_a + \overline{\mu}_a + \overline{\alpha}_a)} \times \frac{b\overline{\beta}_a}{(1-p)\overline{\mu}_v},$$

which is the same obtained by Cruz-Pacheco et al. (2005). The first term of the product is the number of infections produced by a single infectious bird during its effective infectious period when bitten by susceptible mosquitoes. The second term (with $p = 0$) is the number of infections in the susceptible avian population produced by a single infectious mosquito during its lifespan. Vertical transmission increases the output rate in the susceptible class S_a by $p\overline{\mu}_v$, which is the reason why R_0 is increased with p. This product must be greater than one in order to sustain the WNV disease. In Table 2 we present the basic reproductive number R_0 for different avian species.

Fig. 1(a) shows the variation of the threshold value R_0 as a function of the mortality rates of birds and mosquitoes. The epidemic outbreak can be avoided with a minor effort when the mosquito mortality μ_v is increased. Conversely, the parameter μ_a needs more increment to eradicate the disease. The curve of R_0 for the transmission probability rates presents a symmetric behavior, see Fig. 1(b).

If $p = 1$ all the mosquito population becomes infectious (this case is not biologically probable because $p \ll 1$, see Turell et al., 2001; Goddard et al., 2002; Dohm et al., 2002). Two assumptions generated this uncommon behavior: infected mosquitoes reproduce equally as uninfected mosquitoes, and the birth rate is equal to the mortality rate. Hence, the dead infected mosquitoes are

Table 2
The calculated basic reproductive number using the epidemiological and demographic parameters given in Cruz-Pacheco et al. (2005), considering $p = 0.007$, $b = 0.5$ and $m = 5$.

Common name	$\overline{\beta}_a$	$\overline{\beta}_v$	$\overline{\gamma}_a$ (day^{-1})	$\overline{\alpha}_a$ (day^{-1})	$\overline{\mu}_a$ (day^{-1})	$\overline{\mu}_v$ (day^{-1})	R_0
Blue jay	1.0	0.68	0.26	0.15	0.0002	0.06	34.69
Common grackle	1.0	0.68	0.33	0.07	0.0001	0.06	35.64
House finch	1.0	0.32	0.18	0.14	0.0003	0.06	20.88
American crow	1.0	0.5	0.31	0.19	0.0002	0.06	20.97
House sparrow	1.0	0.53	0.33	0.1	0.0002	0.06	25.81
Ring-billed gull	1.0	0.28	0.22	0.1	0.0003	0.06	18.32
Black-billed magpie	1.0	0.36	0.33	0.16	0.0001	0.06	15.37
Fish crow	1.0	0.26	0.36	0.06	0.0002	0.06	12.96

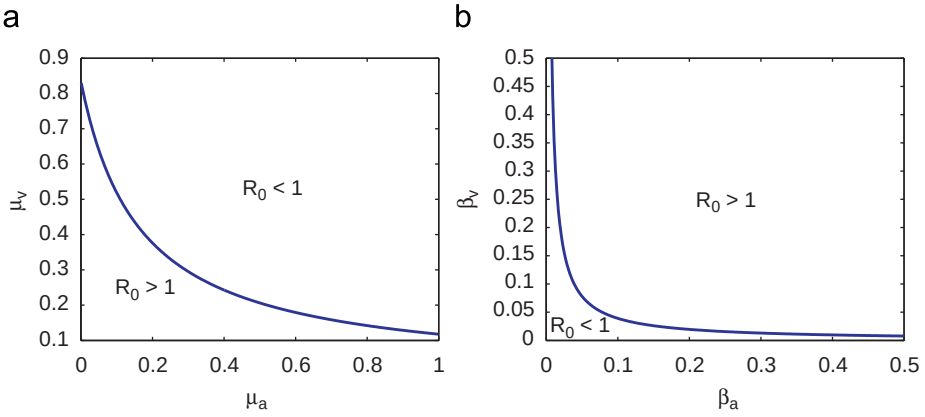

Fig. 1. Graphs for the threshold value R_0, considering (a) the mortality rates and (b) the transmission probability rates, using the blue jay parameters given in Table 2.

completely replenished by the emergence of infected mosquitoes originated from vertical transmission. Hence, the equilibrium point P_1, in the case $p = 1$, is given by

$$S_a^* = \frac{\mu_a - (\gamma_a + \mu_a + \alpha_a)I_a^*}{\mu_a}, \quad I_v^* = 1, \quad N_a^* = \frac{\mu_a - \alpha_a I_a^*}{\mu_a},$$

where I_a^* is the unique positive root in $(0, \mu_a/\mu_a + \alpha_a + \gamma_a)$ of the second degree polynomial

$$r(I_a) = \alpha_a(\alpha_a + \gamma_a + \mu_a)I_a^2 - (\beta_a + \mu_a)(\gamma_a + \mu_a + \alpha_a)I_a + \beta_a\mu_a.$$

The following theorem, which is equivalent to that obtained by Cruz-Pacheco et al. (2005) regarding two equilibrium points, is established:

Theorem 2.1. *If $0 \leqslant p < 1$, then the disease-free equilibrium P_0 is unique and locally asymptotically stable for $R_0 < 1$. When $R_0 > 1$, P_0 becomes unstable, and there appears a new endemic equilibrium P_1 which is locally asymptotically stable. If $p = 1$, P_0 is always unstable, and P_1 is locally asymptotically stable.*

Proof. See Appendix A. □

3. Traveling wave solution

In this section, we study the geographic propagation of WNV using the same methodology applied to describe the dissemination of rabies among foxes (Murray et al., 1986; Murray and Seward, 1992), that is, we determine the minimum wave speed connecting the disease-free equilibrium point to the endemic state. The solution corresponding to the minimum wave speed of the system of equations (6)–(9) describes the observed biological waves (see Sandstede, 2002; Volpert and Volpert, 1994).

The traveling wave solution, when it exists, can be set in the usual form Murray (2002):

$$(s_a(x,t), i_a(x,t), i_v(x,t), n_a(x,t)) = (s_a(z), i_a(z), i_v(z), n_a(z)),$$

where $z = x + ct$. In this new variable, Eqs. (6)–(9) turn into

$$c\frac{ds_a}{dz} = \frac{d^2 s_a}{dz^2} - v_a\frac{ds_a}{dz} + \mu_a - \frac{\beta_a i_v}{n_a}s_a - \mu_a s_a, \tag{15}$$

$$c\frac{di_a}{dz} = \frac{d^2 i_a}{dz^2} - v_a\frac{di_a}{dz} + \frac{\beta_a i_v}{n_a}s_a - (\gamma_a + \mu_a + \alpha_a)i_a, \tag{16}$$

$$c\frac{di_v}{dz} = D\frac{d^2 i_v}{dz^2} - v_v\frac{di_v}{dz} + \beta_v i_a\frac{(1 - i_v)}{n_a} - (1 - p)\mu_v i_v, \tag{17}$$

$$c\frac{dn_a}{dz} = \frac{d^2 n_a}{dz^2} - v_a\frac{dn_a}{dz} + \mu_a - \mu_a\eta_a - \alpha_a i_a. \tag{18}$$

Since diffusion and advection in the avian population are greater than those of the mosquito population, at first we assume that $D = 0$ and $v_v = 0$. Defining the variables $u_1 = ds_a/dz$, $u_2 = di_a/dz$ and $u_3 = dn_a/dz$, the corresponding first-order ordinary differential equations with respect to variable z of system (15)–(18) are

$$\frac{ds_a}{dz} = u_1, \tag{19}$$

$$\frac{du_1}{dz} = (c + v_a)u_1 - \mu_a + \frac{\beta_a i_v}{n_a}s_a + \mu_a s_a, \tag{20}$$

$$\frac{di_a}{dz} = u_2, \tag{21}$$

$$\frac{du_2}{dz} = (c+v_a)u_2 - \frac{\beta_a i_v}{n_a} s_a + (\gamma_a + \mu_a + \alpha_a) i_a, \tag{22}$$

$$\frac{di_v}{dz} = \frac{1}{c}\left[\beta_v i_a \frac{(1-i_v)}{n_a} - (1-p)\mu_v i_v\right], \tag{23}$$

$$\frac{dn_a}{dz} = u_3, \tag{24}$$

$$\frac{du_3}{dz} = (c+v_a)u_3 - \mu_a + \mu_a \eta_a + \alpha_a i_a, \tag{25}$$

where the boundary conditions are

$$\lim_{z\to-\infty} (s_a(z), u_1(z), i_a(z), u_2(z), i_v(z), n_a(z), u_3(z)) = (1,0,0,0,0,1,0) \tag{26}$$

and

$$\lim_{z\to\infty} (s_a(z), u_1(z), i_a(z), u_2(z), i_v(z), n_a(z), u_3(z)) = (S_a^*, 0, I_a^*, 0, I_v^*, N_a^*, 0). \tag{27}$$

The zeros in both equilibrium points deserve some considerations. The three zeros in the second equilibrium point correspond to derivatives of the subpopulations s_a, i_a and n_a. However, the first equilibrium point has two more zeros corresponding to infectious populations regarding birds and mosquitoes, which must not assume negative numbers. Due to this constraint, we impose on the linear system solutions that must not oscillate, i.e., the eigenvalues corresponding to this equilibrium point must assume real values.

The roots of the characteristic polynomial regarding the linear system at the equilibrium point $(s_a, u_1, i_a, u_2, i_v, n_a, u_3) = (1,0,0,0,0,1,0)$ are the roots of the polynomial $Q(\lambda)$ and $P(\lambda)$, where

$$Q(\lambda) = [\lambda^2 - (c+v_a)\lambda - \mu_a]^2 \tag{28}$$

and

$$P(\lambda) = \lambda^3 + A\lambda^2 + B\lambda + C, \tag{29}$$

where the coefficients are

$$A = c + v_a - \frac{\mu_v(1-p)}{c},$$

$$B = -(\alpha_a + \gamma_a + \mu_a) - \frac{\mu_v(c+v_a)(1-p)}{c},$$

$$C = \frac{(1-p)\mu_v(\gamma_a + \mu_a + \alpha_a)}{c}(R_0 - 1)$$

with R_0 being given by (14). The polynomial $Q(\lambda)$ always has real roots. Then the polynomial $P(\lambda)$ must carry the conditions for the existence of minimum speed, that is, the eigenvalues are reals. The minimum velocity (see Appendix B) is determined by the condition that the polynomial evaluated at the unique local minimum, λ_+, must be zero, that is, $P(\lambda_+) = 0$, where

$$\lambda_+ = \tfrac{1}{3}\left\{-A + \sqrt{A^2 - 3B}\right\}.$$

We calculate the non-dimensional c_{min} and the dimensional wave speed, denoted by V_{min}, for eight species of birds, which are given in Table 3, considering $D_a = 6\,\mathrm{km}^2/\mathrm{day}$. We assume that, as in Cruz-Pacheco et al., 2005, the typical value of the biting rate is once every two days, or $b = 0.5$, and the ratio $m = N_v/(\Lambda_a/\mu_a) = 5$. The remaining non-dimensional parameter is $\beta_a = \overline{\beta}_a = 1$. Note that house finch and American crow have quite the same R_0, see Table 2, but the wave speeds assume slightly different values.

Fig. 2 shows the wave speed as a function of the diffusion coefficient for three species of birds: blue jay, common grackle and fish crow. The fish crow presents R_0 lower than the other two species, and the wave speed is considerably lower. Okubo (1998) estimated an interval for this diffusion between 0 and $14\,\mathrm{km}^2/\mathrm{day}$. Considering $p = 0.007$, $D_a = 6\,\mathrm{km}^2/\mathrm{day}$, and $v_a = 0$, we obtain 3.03 km/day as the velocity of disease propagation for blue jay, which falls within the range of 3−3.5 km/day observed in field data (see maps in DeBiasi and Tyler, 2006). If we consider a biting rate of 0.3 (once every three days) as in Lewis et al. (2006), we obtain a wave speed of 1.98 km/day, which is clearly an underestimation. In this case ($b = 0.3$), the observed speed of disease propagation in DeBiasi and Tyler (2006) (3–3.5 km/year) can be obtained when we combine the diffusion and advection movements ($v_a \neq 0$).

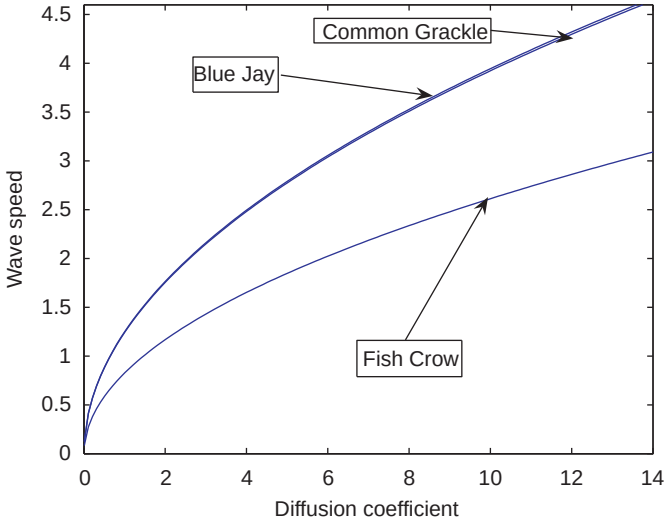

Fig. 2. Graph of the dimensional wave speed as a function of the diffusion coefficient of the avian population D_a, considering $p = 0.007$ and $b = 0.5$. For $D_a = 6\,\mathrm{km}^2/\mathrm{day}$ we observe that the wave speed is approximately 3 km/day for the blue jay and the common grackle. The wave speed is 2.02 km/day for the fish crow. The wave speed varies from 0 to 4.7 km/day for the blue jay and the common grackle, while for the fish crow the wave speed varies from 0 to 3.1 km/day.

Table 3
Values of the non-dimensional parameters used to calculate the minimum wave speeds.

Common name	β_v	γ_a	α_a	μ_a	μ_v	c_{min}	V_{min} (km/day)
Blue jay	0.136	0.104	0.06	0.00008	0.024	0.784	3.03
Common grackle	0.136	0.132	0.028	0.00004	0.024	0.789	3.05
House finch	0.064	0.072	0.056	0.00012	0.024	0.624	2.41
American crow	0.1	0.124	0.076	0.00008	0.024	0.658	2.54
House sparrow	0.106	0.132	0.04	0.00008	0.024	0.705	2.73
Ring-billed gull	0.056	0.088	0.04	0.00012	0.024	0.592	2.29
Black-billed magpie	0.072	0.132	0.064	0.00004	0.024	0.572	2.21
Fish crow	0.052	0.144	0.024	0.00008	0.024	0.522	2.02

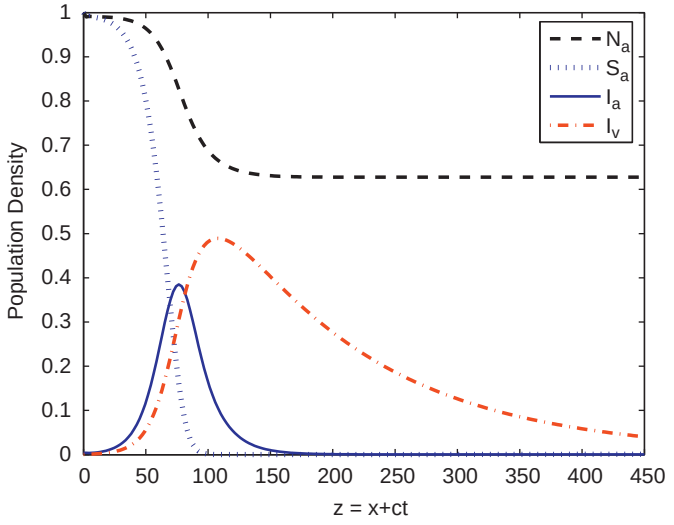

Fig. 3. Traveling wave solution for WNV model, Eqs. (19)–(25), using the non-dimensional parameters with respect to the blue jay listed in Table 3. Advection is not considered ($v_a = 0$). When advection is considered in the direction of the arrow pointed to the left, $v < 0$, the wave speed is increased. For $[t]$ units of time the solution is shifted to the left $c[t]$ units in the space $[x]$ ($z = x + ct$).

Lewis et al. (2006) obtained the wave velocity of 2.74 km/day for $b = 0.3$, assuming that there are neither disease-induced mortality nor recovery rates. However, if we assign values different from zero to both parameters (see Table 2), then the wave velocity decreases to 1.98 km/day. These parameters decrease the value of wave speed.

In Fig. 3 we show the numerical traveling wave solution for the first-order system of equations (19)–(25). We observe the occurrence of the first peak of infection in the four classes.

4. Sensitivity analysis of the wave speed

The wave speed of WNV propagation depends on several parameters, which can vary broadly. We perform the sensitivity analysis of the wave speed with respect to the essential parameters. The sensitivity analysis is performed taking into account the values of the parameters given in Table 3. The advection movement increases the wave speed in the left direction (when $v_a < 0$) and decreases it in the right direction (when $v_a > 0$), therefore we set a null value for it ($v_a = 0$) and, hence, this parameter does not contribute to the sensitivity analysis of the main parameters. Only at the end of this section we study the effects of the advection movement.

4.1. Vertical transmission

Culex pipiens mosquitoes are one of the most important vectors of WNV and present high values for vertical transmission compared with other species of mosquitoes. A rate of 0.62 per 1000 $F1$, the first progeny, i.e., $p = 0.00062$, was estimated (Turell et al., 2001). Dohm et al. (2002) reported a rate of 1.4 per 1000 considering a temperature of 18 °C, and 2.1 for 26 °C. Goddard et al. (2002), however, did not detect vertical transmission. According to our results, the variation observed in vertical transmission in the laboratory experiments is not important because the wave speed does not change considerably with respect to vertical transmission.

By letting $D_a = 6\,\text{km}^2/\text{day}$ and $p = 0$, we have $V_{min} = 3.03\,\text{km/day}$, while for $p = 1$, we have $V_{min} = 3.09\,\text{km/day}$. Considering the extreme value of diffusion $D_a = 14\,\text{km}^2/\text{day}$ and $p = 0$, we have $V_{min} = 4.64\,\text{km/day}$, and for $p = 1$, we have $V_{min} = 4.72\,\text{km/day}$. The wave speed increases approximately 0.06–0.08 km/day (1.7–2.0%) when vertical transmission assumes the lower and the upper bounds. The reason why vertical transmission is not an important factor for spatial dynamics is due to the fact that mosquito movements are negligible compared with avian movements. Another reason arises from the fact that the model disregards the aquatic phase of the mosquito's life cycle and the long distance transport of eggs (especially those infected) due to transportation facilities.

4.2. Recovery rate

Our model encompasses the recovery of the infected avian population, which is not taken into account in Wonham et al. (2004) and Lewis et al. (2006). They considered a null recovery rate ($\gamma = 0$) based on the literature (Work et al., 1955). Recent experiments were carried out to evaluate the transmission dynamics, and Komar et al. (2003) observed the existence of a recovered subpopulation. From 25 species of birds exposed to WNV by the bite of infectious mosquito *C. tritaniorhynchus*, they found that the house finch presented the highest mean duration of infection, 5.5 days ($\overline{\gamma}_a^{-1} = 0.18$); the blue jay presented a mean duration of 3.75 days ($\overline{\gamma}_a^{-1} = 0.26$); and the common grackle, 3 days ($\overline{\gamma}_a^{-1} = 0.33$). According to Fig. 2, the blue jay and the common grackle have quite the same wave speed, but if the recovery rate is not considered ($\overline{\gamma}_a = 0$), then the wave speed increases considerably (see Fig. 4). The recovery rate for the common grackle is higher than that for the blue jay, hence the effect on the increase in the wave speed is higher.

For a value of $D_a = 6\,\text{km}^2/\text{day}$ and $b = 0.5$: (1) for $\overline{\gamma}_a = 0.33$, we have $V_{min} = 3.05\,\text{km/day}$ (1113.25 km/year) and (2) for $\overline{\gamma}_a = 0$, we have $V_{min} = 3.63\,\text{km/day}$ (1325 km/year). Considering $b = 0.3$: (1) for $\overline{\gamma}_a = 0.33$, we have $V_{min} = 2$ km/day (730 km/year) and (2) for

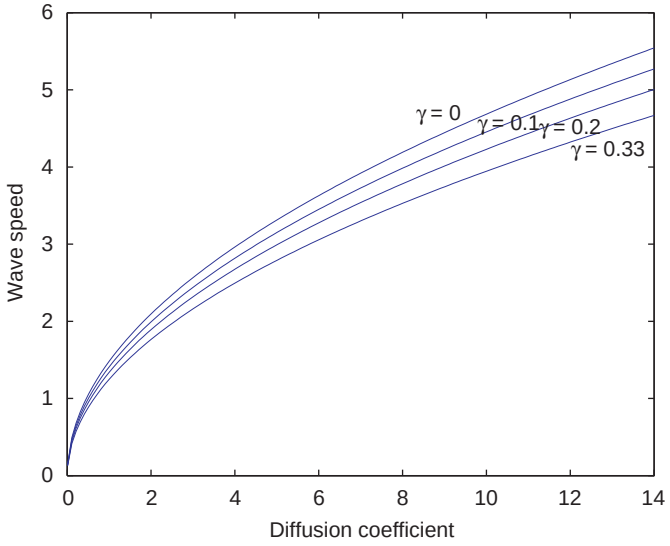

Fig. 4. Graph of the dimensional wave speed V_{min} (km/day) as a function of the diffusion coefficient (km^2/day) for the common grackle considering different dimensional recovery rates ($\overline{\gamma}_a = 0, 0.1, 0.2$ and 0.33). The common grackle has a recovery rate greater than other species. We can observe that the wave speed (curve for $\overline{\gamma}_a = 0.33$) is increased when recovery rate is not considered (curve for $\overline{\gamma}_a = 0$).

$\overline{\gamma}_a = 0$, we have $V_{min} = 2.72$ km/day (992 km/year). The wave speed increases approximately 0.58–0.72 km/day (19.0–36.0%) when the recovery rate is not considered.

4.3. Disease-induced mortality rate

Disease-induced mortality rate was accounted for by the model, while Wonham et al. (2004) and Lewis et al. (2006) did not consider it, letting $\delta = 0$. In Komar et al. (2003), obvious signs of illness were observed in 28 birds among 87 mosquito-exposed birds: an unusual posture (blue jay), inability to hold head upright and ataxia (ring-billed gull). In most cases, clinical signs were followed by death in 24 h.

An increase in disease-induced mortality rate decreases the wave speed because the infected subpopulation decreases. For the blue jay bird parameters, and a value of $D_a = 6\,\text{km}^2/\text{day}$, with $b = 0.5$: (1) for $\alpha_a = 0.15$, we have $V_{min} = 3.03$ km/day (1,106 km/year) and (2) for $\alpha_a = 0$, we have $V_{min} = 3.29$ km/day (1,201 km/year). For $b = 0.3$: (1) for $\alpha_a = 0.15$, we have $V_{min} = 1.98$ km/day and (2) for $\alpha_a = 0$, we have $V_{min} = 2.29$ km/day. The wave speed increases approximately 0.26–0.31 km/day (8.6–15.7%) when disease mortality is not considered.

The variation in wave speed promoted by disease-induced mortality rate ranges between the variations observed in vertical transmission and in the recovery rate.

4.4. Mosquito biting rate

The estimation of biting rate is not an easy task, which is why a very broad range of values is found in the literature. For instance, Cruz-Pacheco et al. (2005) considered one bite every two days, taking $b = 0.5$. Lewis et al. (2006) considered, approximately, one bite every three days, resulting in $b = 0.3$. Wonham et al. (2004) reported on the biting rate of *Culex* spp. mosquitoes among birds and observed that 27% of the bites are on crows and also that female mosquitoes bite once every three days, hence obtaining a mean biting rate of 0.09. Considering these estimations, in Fig. 5 we show the variation of the wave speed (km/day) with respect to the diffusion coefficient (km^2/day) for three different biting rates ($b = 0.5$, 0.3 and 0.1).

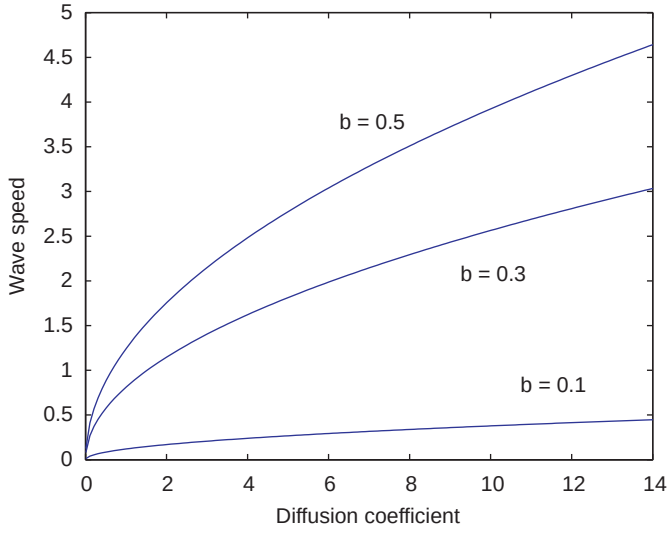

Fig. 5. Graph of the dimensional wave speed V_{min} (km/day) as a function of the diffusion coefficient (km^2/day) for the blue jay considering different biting rates. The wave speed presents a high sensitivity with respect to the biting rate. For the biting rate $b = 0.1$ the wave speed obtained is very low. The biting rate increases the wave speed considerably for $b = 0.3$ and 0.5.

The sensitivity of the wave speed with respect to the biting rate is high. For a mean value of diffusion such as $D_a = 6\,\text{km}^2/\text{day}$ and taking into account the blue jay parameters, we have (1) for $b = 0.5$, $V_{min} = 3.03$ km/day (1,106 km/year), (2) for $b = 0.3$, $V_{min} = 1.98$ km/day (722.7 km/year) and (3) for $b = 0.1$ the value obtained is very low, $V_{min} = 0.29$ km/day (105.85 km/year). In the work of Lewis et al., using $b = 0.3$, they obtained approximately 2.75 km/day for the wave speed, which can be taken as the upper bound since they did not consider the recovery and disease-induced mortality rates. The sensitivity with respect to the biting rate is very high and this parameter must be chosen carefully.

4.5. Diffusion movement

In Fig. 5 we show the effects of diffusion on the wave speed for three different biting rates. We allowed 0 to 14 km^2/day for the range of variation of diffusion movements, according to Okubo (1998). The curve for $b = 0.5$ varies from 0 to 4.7 km/day; for $b = 0.3$ it varies from 0 to 3.03 km/day; and for $b = 0.1$, from 0 to 0.45 km/day. The effect of diffusion on wave speed is imperceptible for lower biting rates. For higher values, an average of $D_a = 6\,\text{km}^2/\text{day}$ (considered in Lewis et al., 2006 and in this work) seems a good approximation.

In Fig. 2 we show the variation of wave speed with respect to diffusion for three species of birds. Blue jay and common grackle, which have the fastest speed, and for fish crow, which has the lowest speed. The variation in wave speed for other species ranges between those curves. The wave speed varies from 0 to 4.7 km/day for the blue jay and for the common grackle. For the fish crow, the wave speed varies from 0 to 3.1 km/day.

4.6. Advection movement

We now take account of the advection movement. A preferential direction (migratory movements) for birds is observed, which goes from New York City to Florida state (north–south). Nevertheless, let us assume an advection movement in the east–west direction to verify if this route of advection is important for disease dissemination from New York to California. Some isolated cases occurred in California in the year 2002, due to long migratory movements of birds, before than the first cases occurred on other states, such as AZ, UT, NV, CR (DeBiasi and Tyler, 2006) (see Fig. 7). The advection movement increases the wave speed in the east–west direction: if we take $v_a < 0$, the speed of wave front increases in the left direction and decreases in the opposite direction. In order to describe the propagation from New York to California, encompassing an east-west direction because the efforts to control the disease must be increased, we analyze the case $v_a < 0$. Considering an average diffusion value $D_a = 6\,\text{km}^2/\text{day}$, and when advection is not considered ($v_a = 0$), we obtained a wave speed of 1.98 km/day for $b = 0.3$, and 0.29 km/day for $b = 0.1$. Then, to achieve the observed value for the wave speed of 3 km/day (DeBiasi and Tyler, 2006), for $b = 0.3$, an advection coefficient of $v = -1.65$ km/day must be introduced, and for $b = 0.1$, a high advection coefficient is needed, $v = -9.2$ km/day.

In Fig. 6(a) and (b), we can observe that the effect of advection is greater for $b = 0.3$ than for $b = 0.1$. For $b = 0.3$ the wave speed increases approximately 4.22 km/day (for all diffusion values), when advection increases from 0 to 6 km/day, see Fig. 6(a). For $b = 0.1$, advection increases the wave speed approximately 1.7 km/day (for all diffusion values), according to Fig. 6(b).

Similarly, in Fig. 6(a) and (b), we can observe that the effect of diffusion is greater for $b = 0.3$ than for $b = 0.1$. The curves are more distant for $b = 0.3$ (Fig. 6(a)) than for $b = 0.1$ (Fig. 6(b)). The

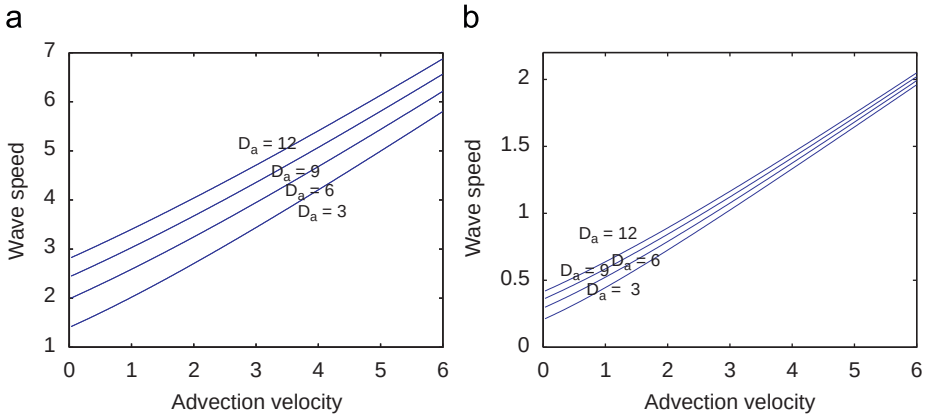

Fig. 6. Graph of the wave speed (km/day) as a function of the absolute value of the advection coefficient (km/day) allowed to the left direction $v_a < 0$, for different diffusion coefficients (km^2/day). When advection increases from 0 to 6 km/day, note that the wave speed increases (a) approximately 4.2 km/day for $b = 0.3$ and (b) approximately 1.7 km/day for $b = 0.1$. The wave speed is more sensitive to advection at higher biting rates.

Fig. 7. (a) WNV begins to propagate from New York in 1999. (b) In the second year the wave front travels 187 km to the north and 1100 km to the south. (c) The wave front travels 1100 km to the west in 2001. (d) The wave front travels 1300 km in 2002, disregarding the isolated cases appeared in California state.

wave speed increases substantially for a biting rate of $b = 0.3$ than for $b = 0.1$. This is in agreement with the diffusion sensitivity analysis, shown in Fig. 5.

Hence, the sensitivity of the wave speed with respect to diffusion and advection is more considerable for $b = 0.3$ than for $b = 0.1$. In both cases, the propagation of WNV disease across the USA can be explained as a combination of diffusion and advection movements. However, for $b = 0.5$, advection is unnecessary.

5. Geographic spreading of WNV

WNV was identified in New York City in 1999, and since then it has propagated to the south and to the east regions of the USA. The front of disease traveled 187 km to the north and 1100 km to the NC state, in the south, in the second year (2000). In the third year (2001), the wave front traveled 312 km to the north (ME state), reaching the border, and traveled 1100 km to the west. In the fourth year (2002), the wave front traveled 1300 km to the west, to the CO and WY states. Some isolated cases appeared in California, but they were not taken into account in the wave speed assessment. In the fifth year (2003), the wave front reached the California state, traveling 1200 km. Fig. 7 shows the propagation of WNV from New York to California state (DeBiasi and Tyler, 2006). In the south and the west directions, the range of the wave speed is 3–3.5 km/day.

If we consider the mean diffusion coefficient for the avian population $D_a = 6$ km/day, the wave speed obtained for $b = 0.3$ is 1.98 km/day (722.7 km/year), i.e., the wave front is underestimated. In this case, we must add an advection velocity in the range of 1.65–2.37 km/day to the south and west, and the speed of the wave front increases to 1100–1300 km/year (3–3.5 km/day).

That range for advection velocity decreases the wave front, in the opposite direction in the range of 319–422 km/year (0.87–1.15 km/day). If we consider $b = 0.1$ and an advection velocity of 2 km/day in the south direction, the wave front is stopped to the backward, that is, WNV disease cannot be disseminated to the north.

Different stopover strategies for refuelling are used by the birds during their migration journeys (Erni et al., 2002). The birds spend some days at the stopover sites, and could disseminate the disease. Small advection of the birds can be considered due to stopover during migration.

Different wave speeds obtained by considering intermediate biting rates and small advection movements can explain the speed of disease dissemination obtained in field data in different directions. The common grackle, one of the most competent birds in disseminating WNV, the American crow, the ring-billed gull and the fish crow, in high densities, follow the southeastern US route. However, between stopover sites, each bird follows its own migration path, so flock membership changes continuously (Rappole et al., 2000). Those behaviors are favorable to the dissemination of WNV disease in the southwest route followed by these birds.

The blue jay, another competent bird in the dissemination of WNV, follows this route of migration. The westward extension in the winter range of the blue jay banded in New York indicates that these birds migrate in a somewhat southwestwardly direction (Stewart, 1982). Another fact that can spread the virus inland, to the west, is the elliptical migration routes used by many songbirds (blue jay, house finch and black-billed magpie). This relatively common pattern concentrates songbirds along the Atlantic seaboard during the fall migration, but more inland during the spring

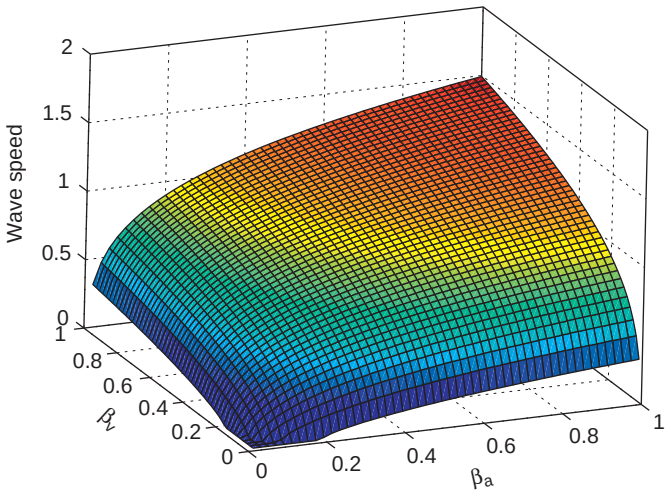

Fig. 8. Non-dimensional wave speed c_{min} as a function of the transmission probabilities for the blue jay parameters with $b = 0.5$. The wave speed is symmetric with respect to the transmission probabilities, because polynomial (29) gives the wave speed and is symmetric with respect to these parameters. When $R_0 < 1$, see Fig. 1 (b), the wave speed is zero.

(Reed et al., 2002). The house sparrow is a resident songbird, and then it is less competent in WNV dissemination.

In the wildlife, different species of mosquitoes and birds coexist. For this reason, we study the effects of transmission probabilities in the avian and mosquito populations on the wave speed.

Fig. 8 shows the variation of the wave speed as a function of transmission probabilities (β_a, β_v), considering the blue jay parameters. When $R_0 < 1$, see Fig. 1, the wave speed is null, and the disease does not propagate. The wave speed is symmetric with respect to transmission probabilities, then the effort to control the disease is the same in the avian and mosquito populations. When probabilities are near 1, the wave speed is near $c_{min} = 1.5$. For $D_a = 6\,\text{km}^2/\text{day}$ and $b = 0.5$, the wave speed is $V_{min} = 5.8$ km/day. This is an upper bound for the wave speed. The upper bound of the range of β_a estimated for the fish crow, the common grackle and the blue jay is less than 1, being $0.052 \leqslant \beta_a \leqslant 0.136$, hence the velocity is less than 3 km/day.

Culex spp. of mosquitoes are likely to play the major role in the enzootic maintenance and transmission of WNV in California. The competence study among 10 Californian species was done in Goddard et al. (2002). For *Culex* spp., except for *Cx. quinqufasciatus*, the infection was between 58% and 100%. However, for *Cx. quinqufasciatus*, the infection rate was lower than 15%. *Cx. tarsalis* was the most efficient vector transmitting the virus in laboratory experiments, near 60%, followed by *Cx. p. quinqufasciatus*, which was infected closely to 52%. *Cx. p. pipiens* showed a moderate transmission rate ranging from 19% to 36%. We calculate the wave speed considering the different transmission rate values (β_a, β_v) presented in that work (Table 4).

When we consider $b = 0.3$, *Cx. tarsalis* and *Cx. p. pipiens* are able to propagate the disease. The wave speed for *Cx. tarsalis* is 1.61 km/day (587.65 km/year), and for *Cx. p. pipiens*, the value obtained is 1.21 km/day (441.65 km/year). *Cx. quinquefasciatus* is not able to propagate the disease. With respect to bird parameters, we considered the values for the blue jay (Table 2).

Comprehensive mosquito surveillance and control plan are done in New York City Department of Health and Mental Hygiene (2004) to avoid WNV disease. It is important to understand the role of the mosquito's mortality rate μ_v in the disease dynamics and, also in the wave speed. Moreover, understanding the role of μ_a is important to predict the spread of the disease before the onset of human illness (New York City Department of Health and Mental Hygiene, 2004). Additionally, reliable assessment of the different mortality rates among birds is important because different species can transmit WNV differently.

Fig. 9 shows the wave speed as a function of mortality rates (μ_a, μ_v), considering the blue jay parameters. Again, when $R_0 < 1$, see Fig. 1, the wave speed is zero. We observe that lower avian mortality values imply higher efforts to control the wave speed. The wave speed c_{min} is in the range of 0–0.798, i.e., for $D_a = 6\,\text{km}^2/\text{day}$ and $b = 0.5$, we have 0–3.09 km/day, an upper bound for the wave speed corresponding to the blue jay, which is 3.03 km/day. If control mechanisms are applied, in order to increase the mosquito's mortality from 0.024 to 0.24, the wave speed decreases from $c_{min} = 0.789$ (3.03 km/day) to $c_{min} = 0.65$

Table 4
Transmission probabilities and vertical transmission parameters for mosquitoes.

Name	β_a	β_v	p	b	V_{min} (km/day)	b	V_{min} (km/day)
Culex tarsalis	0.65	0.75	0.007	0.5	2.59	0.3	1.61
Cx. p. pipiens	0.28	1.0	0.002	0.5	2.1	0.3	1.21
Cx. p. quinquefasciatus	0.52	0.1	0.003	0.5	0.71	0.3	–

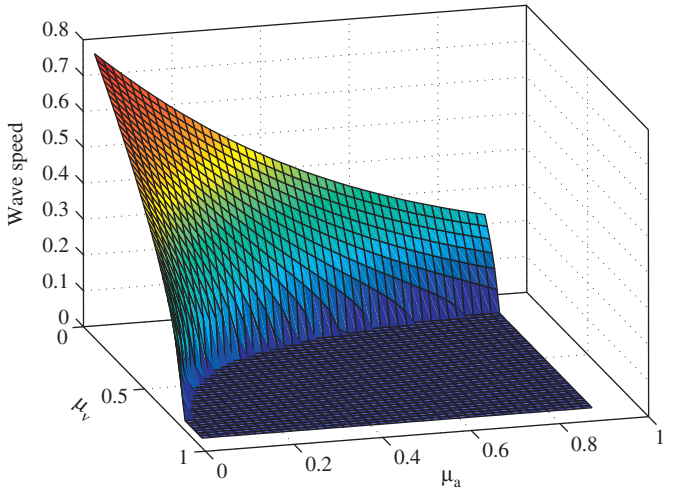

Fig. 9. Non-dimensional wave speed c_{min} as a function of the mortality rates for the blue jay parameters with $b = 0.5$. When $R_0 < 1$, see Fig. 1(a), the wave speed is zero. We can observe that in this case the wave speed is not symmetric. Assuming that the mosquito population is constant, mosquito control is efficient to reduce the disease propagation.

(2.5 km/day). Higher avian mortality values μ_a provide a more efficient mosquito control.

Note that higher values for mosquito mortality rate decrease the wave speed more than do higher avian mortality values, although the movement is considered only in the avian population. This fact arises because the infected avian subpopulation is not reduced only by avian mortality, but also by disease-induced mortality and by the recovery rates. Vertical transmission is not a considerable factor of WNV propagation for lower mosquito mortality rate values. A higher vertical transmission value has more effect on wave speed when high mosquito birth and mortality (μ_v) rates are considered at the same time. This fact is due to the expression of R_0 having the term $(1-p)\mu_v$ in the denominator. The biological meaning is that vertical transmission supplies the infected mosquito subpopulation with more individuals than does the infection occurring among susceptible individuals, and due to the fact that the entire population is constant in this model, the increase in mortality rate μ_v increases the birth rate equally.

Let us assess the effects of mosquito movements (diffusion and/or advection) on the wave speed ($D \neq 0$ or/and $v_v \neq 0$). As was done in Section 3, we study the existence of traveling wave solution for the system of equations (15)–(18) by analyzing the corresponding first-order system of equations given in Appendix B.

The roots of the characteristic polynomial corresponding to the linear system at the equilibrium point $(s_a, u_1, i_a, u_2, i_v, u_3, n_a, u_4) = (1, 0, 0, 0, 0, 0, 1, 0)$ are given by the roots of $Q(\lambda) \times T(\lambda)$, where

$$Q(\lambda) = [\lambda^2 - (c + v_a)\lambda - \mu_a]^2 \tag{30}$$

and

$$T(\lambda) = -E\lambda^4 + F\lambda^3 + G\lambda^2 + H\lambda + J, \tag{31}$$

where the coefficients are

$$E = \frac{D}{c},$$

$$F = \frac{c + v_v + D(c + v_a)}{c},$$

$$G = \frac{(c + v_a)(c + v_v) - \mu_v(1 - p)}{c},$$

$$H = \frac{-(c + v_v)(\alpha_a + \gamma_a + \mu_a) - \mu_v(c + v_a)(1 - p)}{c},$$

$$J = \frac{(1 - p)\mu_v(\gamma_a + \mu_a + \alpha_a)}{c}(R_0 - 1)$$

with R_0 given by (14). The polynomial $Q(\lambda)$ is the same as in the case $D = 0$ and always has real roots. Then the polynomial $T(\lambda)$ must carry the conditions for the existence of the minimum speed. Again, the equation to obtain the minimum velocity results from the condition that the polynomial evaluated at the unique local minimum, λ_+^1, must be zero, that is, $T(\lambda_+^1) = 0$ (see Appendix B).

Note that when the diffusion and advection movements of mosquitoes are not considered ($D = 0$ and $v_v = 0$), the polynomial $T(\lambda) = P(\lambda)$, that is, the wave speed is the same. When the diffusion and advection movements are considered, an increase in the wave speed is obtained.

When we consider the parameters for the blue jay with $b = 0.5$, without mosquito movements ($D_v = 0$), we obtain a non-dimensional wave speed $c_{min} = 0.784$. For $D_a = 6\,\text{km}^2/\text{day}$, the dimensional wave is $V_{min} = 3.03\,\text{km/day}$. If we allow for diffusion movement in the mosquito population, a value of $D_v = 0.02\,\text{km}^2/\text{day}$, Harrington et al. (2005), we have $D = D_v/D_a = 0.02/6$, and the non-dimensional wave speed obtained is $c_{min} = 0.785$. For dimensional parameters, the wave speed is $V_{min} = 3.04$ km/day. When we decrease the biting rate to $b = 0.3$, for $D = 0$, the non-dimensional wave speed is $c_{min} = 0.662$, i.e., $V_{min} = 1.98\,\text{km/day}$. When the diffusion movement of mosquitoes is considered, we have $D = 0.02/6$, and the wave speed is increased to $c_{min} = 0.663$, i.e., $V_{min} = 1.99\,\text{km/day}$. The diffusion movement of mosquitoes is not a significant factor in the spread of WNV.

When the advection movement of the mosquito population is considered, an average value of $\bar{v}_v = 0.05\,\text{km/day}$, the wave speed increases from 3.04 km/day (without advection) to 3.06 km/day for a biting rate of $b = 0.5$, and from 1.99 km/day to 2.01 km/day for a biting rate of $b = 0.3$. The transport and the diffusion movements of mosquitoes are not important in WNV dissemination, in opposition to bird movements, which are the dominant parameters in the variation of the wave speed of disease dissemination.

6. Numerical estimation of the wave speed

Finally, numerical simulations were performed (FlexPDE, 2005), using the non-dimensional system corresponding to the dimensional system of equations (1)–(5) and the dimensional parameters given in Table 2, plus the dimensional parameters $D_a = 6\,\text{km/day}$ for bird diffusion. The remaining parameter v_a, bird advection, is allowed to vary. We do not consider diffusion and advection movements, $D_v = v_v = 0$, because they have little effect on the wave speed. The initial and boundary conditions are given by

$$I_a(x, 0) = \begin{cases} 1, & |x| \leqslant 1/2, \\ 0, & |x| > 1/2 \end{cases} \tag{32}$$

and

$$\bar{S}_a(x, 0) = N_a^0, \quad \bar{R}_a(x, 0) = 0, \quad \bar{N}_a(x, 0) = N_a^0,$$

$$\bar{S}_v(x, 0) = N_v^0, \quad \bar{I}_v = 0. \tag{33}$$

These conditions portray the local introduction of one infectious bird in a disease-free region. For the boundaries, we apply the null

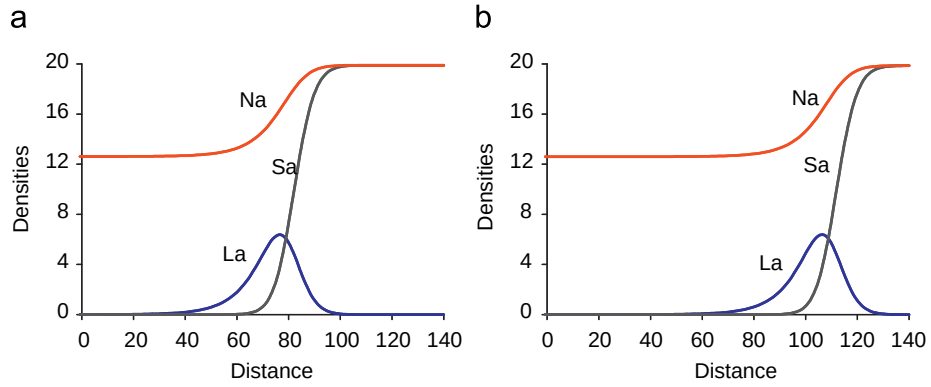

Fig. 10. Traveling wave solution of the PDE system (1)–(5) for the parameters listed in Table 2 for the blue jay, considering $D_a = 6\,\mathrm{km}^2/\mathrm{day}$ and $\overline{v_a} = 0$. The initial and boundary conditions are given by (32)–(33), considering the introduction of one infected bird in a disease-free region. In this case, mosquitoes are not allowed advection and diffusion movements. (a) On day 34.5 the wave traveled 100 km. (b) On day 44.5 the wave traveled 130.3 km, i.e., the wave front traveled at the speed of 3.03 km/day. In the left direction, the wave speed is the same, because advection is not considered neither in birds nor in mosquitoes, hence the graph is symmetric with respect to the ordinate axis.

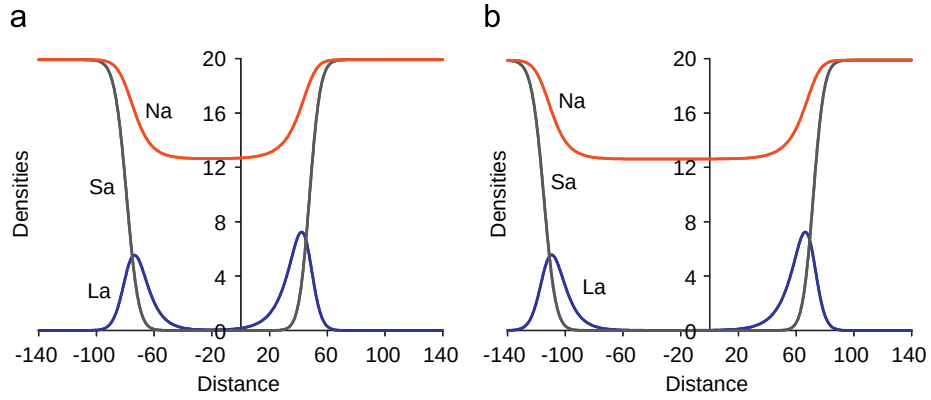

Fig. 11. Traveling wave solution of the PDE system (1)–(5) for the parameters listed in Table 2 for the blue jay, considering $D_a = 6\,\mathrm{km}^2/\mathrm{day}$ and $\overline{v_a} = -1\,\mathrm{km/day}$. The initial and boundary conditions are given by (32) and (33), considering the introduction of one infected bird in a disease-free region. (a) On day 28 the wave traveled 100 km to the left and 68 km to the right. (b) On day 38 the wave traveled 137 km to the left and 90 km to the right. The wave front traveled at a speed of 3.7 km/day to the left and 2.4 to the right. In the left direction, the wave speed is increased by bird advection $\overline{v_a} = -1 < 0$, and the graph is not symmetric in this case with respect to the ordinate axis.

Neumann conditions:

$$\frac{\partial \overline{S}_a}{\partial x}(\pm L, t) = \frac{\partial \overline{I}_a}{\partial x}(\pm L, t) = \frac{\partial \overline{R}_a}{\partial x}(\pm L, t) = \frac{\partial \overline{N}_a}{\partial x}(\pm L, t) = 0,$$

$$\frac{\partial \overline{S}_v}{\partial x}(\pm L, t) = \frac{\partial \overline{I}_v}{\partial x}(\pm L, t) = 0, \quad t > 0. \tag{34}$$

We consider an initial population of 100 mosquitoes and 20 birds per km, i.e., $m = N_v^0/N_a^0 = 100/20 = 5$.

In Fig. 10 we show the disease dissemination when one infected bird is introduced in a completely susceptible population of mosquitoes and birds. The values of the parameters are those given in Table 2 for the blue jay. Fig. 10(a) and (b) shows the propagation of the first wave of epidemics (for the bird population) at two times. On day 34.5 the wave front traveled 100 km. Ten days later, the wave front traveled 130.3 km. Hence, the front wave epidemic traveled at speed $V = (130.3\,\mathrm{km} - 100\mathrm{km})/(44.5\,\mathrm{day} - 34.5\,\mathrm{day}) = 3.03\,\mathrm{km/day}$, which is in agreement with the non-dimensional wave speed $c_{min} = 0.78$ calculated with polynomial (29). This wave speed, obtained with a biting rate equal to $b = 0.5$, is near the front speed obtained from field data (DeBiasi and Tyler, 2006). We remark that we did not consider the advection movement of birds.

In Fig. 11 we show the disease propagation when one infected bird is introduced in a completely susceptible population. In this case, bird diffusion and advection are considered, assuming the values $D_a = 6\,\mathrm{km}^2/\mathrm{day}$ and $\overline{v_a} = -1\,\mathrm{km/day}$ (preferential direction is to the left). Fig. 11(a) and (b) shows the propagation of the first wave of epidemics two times. In this case, the wave front traveled 100 km to the left on the 28th day, earlier than the case without bird advection. Ten days later, the wave front traveled 137 km. Hence, the front wave of the epidemic traveled at speed $V = (137\,\mathrm{km} - 100\,\mathrm{km})/(38\,\mathrm{day} - 28\,\mathrm{day}) = 3.7\,\mathrm{km/day}$. In the right direction, the front wave traveled at the speed of 2.4 km/day. These wave speed values are consistent with the dimensional wave speeds calculated with polynomial (29), considering an advection to the left direction.

7. Conclusion

In this paper, we developed and analyzed a spatial propagation model to understand the dissemination of WNV. For the spatially homogeneous dynamics we determined, in non-dimensional parameters, the threshold value:

$$R_0 = \frac{\beta_a \beta_v}{(1-p)\mu_v(\gamma_a + \mu_a + \alpha_a)},$$

which is the same obtained in Cruz-Pacheco et al. (2005). When R_0 is greater than 1, the endemic state of the disease exists. We study the wave speed for the traveling waves by connecting this endemic point with the disease-free equilibrium point. An equation for the minimum speed was determined as a function of the parameters of the model and the threshold R_0.

The speed of the epidemic waves was assessed with respect to the model's parameters. The dependence of the wave speed on vertical transmission was studied. As the movement of mosquitoes is smaller than that of birds, we obtained that vertical transmission is not an important factor for spatial propagation.

The wave speed was studied as a function of avian diffusion, without advection. Choosing $D_a = 6\,\mathrm{km}^2/\mathrm{day}$, which corresponds to the average value in the range estimated by Okubo (1998) for avian diffusion, we obtained wave speeds of 3.03 km/day for a biting rate of $b = 0.5$ and of 1.98 km/day for $b = 0.3$.

The speed obtained by Lewis et al. (2006) for $b = 0.3$, and from a simplified model that disregarded vertical transmission, the WNV death rate and the avian recovered subpopulation, was 2.74 km/day. This is higher than 1.98 km/year, which was obtained considering the recovery and the avian disease-induced mortality rates. Hence, both parameters play an important role in the transmission dynamics, decreasing the wave speed. Different biting rates were considered in previous works (Cruz-Pacheco et al., 2005; Wonham et al., 2004; Lewis et al., 2006). The wave speed shows high sensitivity with respect to these parameters, telling us that these parameters must be estimated with accuracy.

For $b = 0.3$ we estimated the wave speed as 1.98 km/day, which is an underestimation of the observed wave speed ranging between 3–3.5 km/day (see maps in DeBiasi and Tyler, 2006 and Fig. 7). In order to be comparable with the field data, advection must be considered, which must be fall within the range of 1.65–2.37. The propagation from New York City to California state can be explained by a combination of bird diffusion (random) and advection (preferential direction) movements. The mosquito movements (advection and diffusion) do not play an important role in the increase in the wave speed. We stress that no advection is needed for $b = 0.5$, and that the diffusion movement alone explains the WNV disease dissemination.

For intermediate values of the biting rate b, relatively small advective movements must be added to the high diffusion coefficient to explain the wave speed observed in the field data. The field data showed the same speed of WNV dissemination in both south and west directions from New York City. In the model we considered only small advective movements to describe stopover during long migratory routes.

The common grackle, the American crow, the ring-billed gull, the fish crow and the blue jay are competent birds in disseminating WNV (see Table 3). They follow a route of migration in a somewhat southwestwardly direction (Stewart, 1982). Another fact that can spread the virus inland, to the west, is the elliptical migration routes used by many songbirds (blue jay, house finch and black-billed magpie). This relatively common pattern concentrates songbirds along the Atlantic seaboard during the fall migration, but more inland during the spring (Reed et al., 2002). The house sparrow is a resident songbird, and then it is less competent for the spatial WNV dissemination.

The wave speed of WNV propagation was obtained and analyzed by taking into account only one species of bird. The coexistence of many species of birds with different diffusion movements and competence for WNV transmission, which were not considered in the literature yet, can be another important factor to increase the wave velocity, and must be considered in the modeling. In a future paper, we will analyze the effects of several species of birds on the transmission dynamics and on the wave speed, in order to determine the efficacy of control strategies.

Acknowledgments

We thank the comments and suggestions provided by anonymous referees, which contributed to improving this paper.

Appendix A. Stability analysis of the equilibrium points

In this section we analyze the stability of the equilibrium points.

A.1. Stability of $P_0 = (1, 0, 0, 1)$

By linearizing system (10)–(13) at the equilibrium point P_0, for $p < 1$, we obtain the Jacobian matrix:

$$J(P_0) = \begin{pmatrix} -\mu_a & 0 & -\beta_a & 0 \\ 0 & -\mu_a + \gamma_a + \alpha_a & \beta_a & 0 \\ 0 & \beta_v & -(1-p)\mu_v & 0 \\ 0 & -\alpha_a & 0 & -\mu_a \end{pmatrix}.$$

The eigenvalues are $-\mu_a$ with multiplicity two, and the roots of the polynomial:

$$p_1(\lambda) = \lambda^2 + [\alpha_a + \gamma_a + \mu_a + (1-p)\mu_v]\lambda + (\alpha_a + \gamma_a + \mu_a)(1-p)\mu_v(1 - R_0).$$

All the coefficients of the polynomial $p_1(\lambda)$ are positive if and only if $R_0 < 1$. Therefore, P_0 is locally asymptotically stable if $R_0 < 1$ and is unstable if $R_0 > 1$.

When $p = 1$ the eigenvalues are $-\mu_a$ with multiplicity two, and the roots of the polynomial:

$$p_1(\lambda) = \lambda^2 + (\alpha_a + \gamma_a + \mu_a)\lambda - \beta_a\beta_v.$$

Since the latter coefficient is less than zero, then for $p = 1$ the equilibrium point P_0 is always unstable.

A.2. Stability of $P_1 = (S_a^*, I_a^*, I_v^*, N_a^*)$

The non-trivial equilibrium point P_1 exists if and only if $R_0 > 1$. This condition implies that $S_a^* \geqslant 0$, $I_a^* \geqslant 0$, $I_v^* \geqslant 0$ and $N_a^* \geqslant 0$. The local stability is determined by the roots of $\mathrm{Det}(\lambda Id - J(P_1))$ given by

$$\begin{vmatrix} \lambda + \frac{\beta_a I_v^*}{N_a^*} + \mu_a & 0 & \frac{\beta_a S_a^*}{N_a^*} & -\frac{\beta_a S_a^* I_v^*}{(N_a^*)^2} \\ -\frac{\beta_a I_v^*}{N_a^*} & \lambda + \mu_a + \gamma_a + \alpha_a & -\frac{\beta_a S_a^*}{N_a^*} & \frac{\beta_a S_a^* I_v^*}{(N_a^*)^2} \\ 0 & -\frac{\beta_v(1-I_v^*)}{N_a^*} & \lambda + \frac{\beta_v I_a^*}{N_a^*} + (1-p)\mu_v & \frac{\beta_v(1-I_v^*)I_a^*}{(N_a^*)^2} \\ 0 & \alpha_a & 0 & \lambda + \mu_a \end{vmatrix},$$

where Id is a 4×4 identity matrix. Adding the second row of $(\lambda Id - J(P_1))$ to the first one and using the equalities in the equilibrium:

$$\begin{aligned} \alpha_a + \gamma_a + \mu_a &= \frac{\beta_a S_a^* I_v^*}{I_a^* N_a^*}, \\ \frac{\beta_v I_a^*}{N_a^*} + (1-p)\mu_v &= \frac{\beta_v I_a^*}{N_a^* I_v^*} \end{aligned} \tag{35}$$

we obtain the equivalent matrix:

$$\begin{vmatrix} \lambda+\mu_a & \lambda+\frac{\beta_a S_a^* I_v^*}{I_a^* N_a^*} & 0 & 0 \\ -\frac{\beta_a I_v^*}{N_a^*} & \lambda+\frac{\beta_a I_v^* S_a^*}{I_a^* N_a^a} & -\frac{\beta_a S_a^*}{N_a^*} & \frac{\beta_a S_a^* I_v^*}{(N_a^*)^2} \\ 0 & -\frac{\beta_v(1-I_v^*)}{N_a^*} & \lambda+\frac{\beta_v I_a^*}{I_v^* N_a^*} & \frac{\beta_v(1-I_v^*)I_a^*}{(N_a^*)^2} \\ 0 & \alpha_a & 0 & \lambda+\mu_a \end{vmatrix}.$$

Then, the roots of $\mathrm{Det}(\lambda Id - J(P_1))$ are $-\mu_a$, and the roots of

$$p_2(\lambda) = \lambda^3 + a_2\lambda^2 + a_1\lambda + a_0,$$

where

$$\begin{aligned} a_2 &= \frac{\mu_a}{S_a^*} + \frac{\beta_a I_v^* S_a^*}{I_a^* N_a^*} + \frac{\beta_v I_a^*}{I_v^* N_a^*} > 0, \\ a_1 &= \frac{\mu_a\beta_b I_a^*}{S_a^* I_v^* N_a^*} + \frac{\beta_a\beta_v S_a^* I_v^*}{(N_a^*)^2} + \frac{\beta_a I_v^*(\mu_a N_a^* - \alpha_a I_a^* S_a^*)}{I_a^*(N_a^*)^2}, \\ a_0 &= \frac{\mu_a\beta_v\beta_a\mu_a(N_a^* - S_a^*)}{(N_a^*)^3} + \frac{\mu_a\beta_a\beta_v S_a^* I_v^*}{(N_a^*)^3} - \frac{\alpha_a\beta_a\beta_v S_a^* I_a^*}{(N_a^*)^3}. \end{aligned} \tag{36}$$

From the Routh–Hurwitz criterion, it follows that all the eigenvalues have a negative real part if and only if, $a_2>0$, $a_0>0$ and $a_2a_1>a_0$. Trivially, we have $a_2>0$.

Using $N_a^* - S_a^* = ((\gamma_a+\mu_a)I_a^*)/\mu_a$, a_0 becomes

$$a_0 = \frac{\beta_a\beta_v I_a^*[(\gamma_a+\mu_a) - \alpha_a S_a^*]}{(N_a^*)^3} + \frac{\alpha_a\beta_a\beta_v S_a^* I_a^*}{(N_a^*)^3}. \tag{37}$$

Using the equilibrium point $s_a^* = (1-(\gamma_a+\mu_a+\alpha_a)I_a^*)/\mu_a$, we have

$$\begin{aligned} a_0 = {} & \frac{\beta_a\beta_v I_a^*\left[(\gamma_a+\mu_a-\alpha_a) + \alpha_a\frac{(\gamma_a+\mu_a+\alpha_a)I_a^*}{\mu_a}\right]}{(N_a^*)^3} \\ & + \frac{\beta_a\beta_v S_a^* I_v^*}{(N_a^*)^3} > 0 \end{aligned}$$

because we assumed that $\alpha_a<\gamma_a+\mu_a$ as in Cruz-Pacheco et al. (2005). Finally, we have

$$\begin{aligned} a_2a_1 &> \frac{\beta_v I_a^*}{I_v^* N_a^*}\frac{\beta_a I_v^*(\mu_a N_a^* - \alpha_a I_a^* S_a^*)}{I_a^*(N_a^*)^2} + \frac{\beta_a I_v^* S_a^*}{I_a^* N_a^*}\frac{\mu_a\beta_v I_a^*}{S_a^* I_v^* N_a^*} \\ &> \frac{\beta_v\beta_a\mu_a N_a^*}{(N_a^*)^3} + \frac{\beta_a\beta_v\mu_a S_a^* I_v^*}{N_a^*(N_a^*)^2\times 1} - \frac{\alpha_a\beta_a\beta_v S_a^* I_a^*}{(N_a^*)^3} \\ &> \frac{\beta_v\beta_a\mu_a(N_a^* - S_a^*)}{(N_a^*)^3} + \frac{\beta_a\beta_v\mu_a S_a^* I_v^*}{(N_a^*)^3} - \frac{\alpha_a\beta_a\beta_v S_a^* I_a^*}{(N_a^*)^3} = a_0. \end{aligned}$$

Then in the case $p<1$, the equilibrium point P_1 is locally asymptotically stable if and only if $R_0>1$.

For $p=1$ the eigenvalues are $-\mu_a$, $\beta_v I_a^*/N_a^*$ and the roots of the polynomial

$$\begin{aligned} p_3(\lambda) = {} & \lambda^2 + \left(\frac{\beta_a}{N_a^*} + 2\mu_a + \gamma_a + \alpha_a\right)\lambda \\ & + (\alpha_a+\gamma_a+\mu_a)\left[\frac{\beta_a}{N_a^*} + \mu_a + \alpha_a\frac{\beta_a S_a^*}{(N_a^*)^2}\right]. \end{aligned}$$

All the coefficients of p_3 are positive, then P_1 is always stable.

Appendix B. Traveling waves

In this section, we present the analysis of the speed of the traveling wave solutions.

B.1. Wave speed for the case without mosquito movements

By linearizing the system of first-order system corresponding to Eqs. (19)–(25) at the equilibrium point $(1,0,0,0,0,1,0)$, we obtain the Jacobian matrix:

$$J = \begin{pmatrix} 0 & 1 & 0 & 0 & 0 & 0 & 0 \\ \mu_a & c+v_a & 0 & 0 & \beta_a & 0 & 0 \\ 0 & 0 & 0 & 1 & 0 & 0 & 0 \\ 0 & 0 & \mu_a+\gamma_a+\alpha_a & c+v_a & -\beta_a & 0 & 0 \\ 0 & 0 & \frac{\beta_v}{c} & 0 & -\frac{\mu_v(1-p)}{c} & 0 & 0 \\ 0 & 0 & 0 & 0 & 0 & 0 & 1 \\ 0 & 0 & \alpha_a & 0 & 0 & \mu_a & c+v_a \end{pmatrix}$$

The roots of the characteristic polynomial are the roots of $Q(\lambda)\times P(\lambda)$, where $Q(\lambda)$ and $P(\lambda)$ are given by (28) and (29). The polynomial $Q(\lambda)$ always has two double real roots:

$$\lambda_{1,2} = \tfrac{1}{2}\{c+v_a + \sqrt{(c+v_a)^2+4\mu_a}\}$$

and

$$\lambda_{3,4} = \tfrac{1}{2}\{c+v_a - \sqrt{(c+v_a)^2+4\mu_a}\}.$$

For the polynomial $P(\lambda)$, in the case when we assume the existence of the endemic state, i.e., $R_0>1$, we have

$$P(0) = \frac{(1-p)\mu_v(\gamma_a+\mu_a+\alpha_a)}{c}(R_0-1) > 0.$$

Moreover, it is easy to verify that

$$\begin{aligned} \lim_{\lambda\to\pm\infty} P(\lambda) = \pm\infty, \quad & \left.\frac{dP(\lambda)}{d\lambda}\right|_{\lambda=0} \\ & = -(\alpha_a+\gamma_a+\mu_a) - \frac{\mu_v(c+v_a)(1-p)}{c} < 0, \end{aligned}$$

which implies that $P(\lambda)$ always has one negative real root.

The remaining two roots can be either positive real or complex numbers. In order to obtain the minimum wave speed, we determine the condition such that the imaginary part of the complex root must be zero (or, the roots must be real numbers).

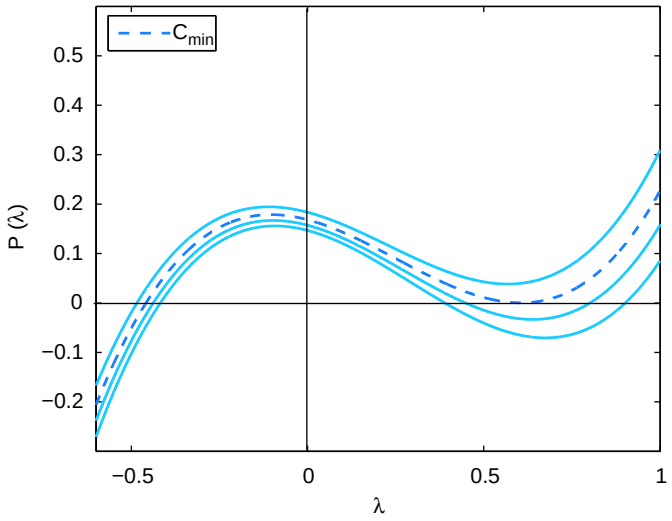

Fig. 12. Graph of the polynomial $P(\lambda)$ for different values of the parameter c. For $c=0.72$, we have only one real root; for $c_{min}=0.78$, a double real root; and for $c=0.84$ and 0.9, three real roots, taking into account the non-dimensional parameters corresponding to those given in table non-dimensional parameters for the blue jay, with $p=0.007$ and $v_a=0$.

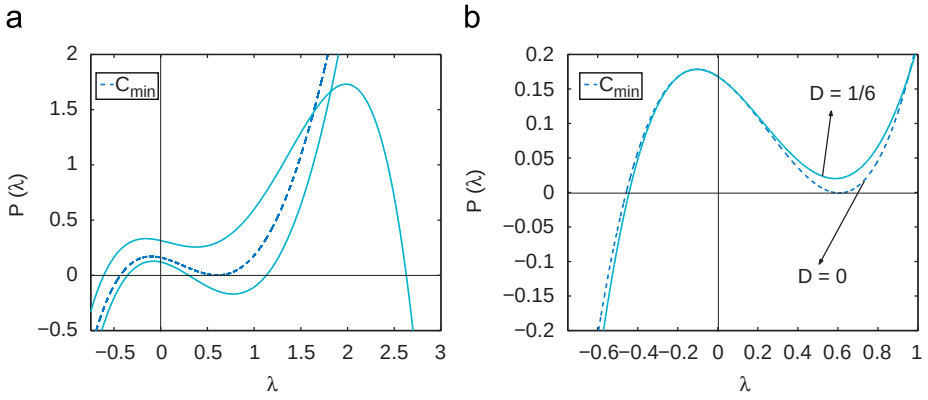

Fig. 13. Graph obtained using the parameters for the blue jay given in Table 3 and $v_a = v_v = 0$. (a) Graph of the polynomial $T(\lambda)$ for different values of the parameter c, considering $D = 1/6$. For $c = 0.42$, we have only one positive real root, only one negative real root and two conjugate complex roots; for $c_{min} = 0.82$, a double real root; and for $c = 1.1$, four real roots. (b) Graph of the polynomial $T(\lambda)$ considering $c = 0.78$. For $D = 0$, the polynomial T is equal to P, and we have the double root because 0.78 is the c_{min}. When $D = 1/6$ we have two conjugate complex roots. The value of c must be increased from 0.78 to 0.82 in order to obtain the double real root, i.e., the minimum speed.

This condition is satisfied when the positive real roots are equal, from which we determine the wave speed (see Fig. 12). The condition to obtain the double roots follows an easy calculation: the polynomial evaluated at the unique local minimum, λ_+, is zero, that is, $P(\lambda_+) = 0$, where

$$\lambda_+ = \tfrac{1}{3}\{-A + \sqrt{A^2 - 3B}\}.$$

B.2. Wave speed for the case considering diffusion and advection in the mosquito population

To establish the traveling wave solution we analyze the following first-order system of equations:

$$\frac{ds_a}{dz} = u_1, \tag{38}$$

$$\frac{du_1}{dz} = (c + v_a)u_1 - \mu_a + \frac{\beta_a i_v}{n_a} s_a + \mu_a s_a, \tag{39}$$

$$\frac{di_a}{dz} = u_2, \tag{40}$$

$$\frac{du_2}{dz} = (c + v_a)u_2 - \frac{\beta_a i_v}{n_a} s_a + (\gamma_a + \mu_a + \alpha_a)i_a, \tag{41}$$

$$\frac{di_v}{dz} = u_3, \tag{42}$$

$$\frac{du_3}{dz} = \frac{1}{D}\left[(c + v_v)u_3 - \beta_v i_a \frac{(1 - i_v)}{n_a} + (1 - p)\mu_v i_v\right], \tag{43}$$

$$\frac{dn_a}{dz} = u_4, \tag{44}$$

$$\frac{du_4}{dz} = (c + v_a)u_4 - \mu_a + \mu_a \eta_a + \alpha_a i_a, \tag{45}$$

where the boundary conditions are

$$\lim_{z\to-\infty}(s_a(z), u_1(z), i_a(z), u_2(z), i_v(z), u_3(z), n_a(z), u_4(z)) = (1, 0, 0, 0, 0, 0, 1, 0) \tag{46}$$

and

$$\lim_{z\to\infty}(s_a(z), u_1(z), i_a(z), u_2(z), i_v(z), u_3(z), n_a(z), u_4(z)) = (S_a^*, 0, I_a^*, 0, I_v^*, 0, N_a^*, 0). \tag{47}$$

When $D \neq 0$ and $v_v = 0$, the characteristic polynomial has the roots given by $Q(\lambda) \times T(\lambda)$, where $Q(\lambda)$ and $T(\lambda)$ are given by (30) and (31). The polynomial $Q(\lambda)$ is the same as for $D = 0$ and $v_v = 0$, and has then always two double real roots.

For the fourth-degree polynomial $T(\lambda)$, in the case where we assume the existence of the endemic state, i.e., $R_0 > 1$, we have (as in the case $D = 0$ and $v_v = 0$)

$$T(0) = (1 - p)\mu_v(\gamma_a + \mu_a + \alpha_a)(R_0 - 1) > 0$$

and

$$\lim_{\lambda\to-\infty} T(\lambda) = -\infty, \quad \left.\frac{dT(\lambda)}{d\lambda}\right|_{\lambda=0} = -c(\alpha_a + \gamma_a + \mu_a) - \mu_v(c + v_a)(1 - p) < 0,$$

which implies that $T(\lambda)$ always has one negative real root.

The new fact for this fourth-degree polynomial is

$$\lim_{\lambda\to+\infty} T(\lambda) = -\infty,$$

which implies that $T(\lambda)$ always has one positive real root.

The remaining two roots can be either positive or conjugate complex roots. As in the case $D = 0$ and $v_v = 0$, the condition that determines the wave speed is $T(\lambda_+^1) = 0$, the polynomial evaluated at the unique local minimum (see Fig. 13).

In Fig. 13(a) we show the polynomial $T(\lambda)$ for different values of c. The curves of the polynomial have four roots, two of which are always real numbers, one negative and the other positive. As in the case $D = 0$ and $v_v = 0$, the wave speed is determined when we have the double real roots evaluated at the local minimum. For $D = 1/6$ and $v_v = 0$, this value is $c = 0.82$. In Fig. 13(b) we fix the value $c = 0.78$. When we consider $D = 0$, we have a double root, because this is the wave speed when the mosquito movements are not considered. When diffusion is considered, with a value of $D = 1/6$, we have two conjugate complex roots, and the value of c must be increased ($c = 0.82$) to obtain the double root. That is, mosquito diffusion increases the wave speed.

References

Bowman, C., Gumel, A.B., Van den Driessche, P., Wu, J., Zhu, H., 2005. A mathematical model for assessing control strategies against West Nile virus. Bulletin of Mathematical Biology 67, 1107–1133.

Campbell, L.G., Martin, A.A., Lanciotti, R.S., Gubler, D.J., 2002. West Nile Virus. The Lancet Infectious Diseases 2, 519–529.

Cruz-Pacheco, G., Esteva, L., Montaño-Hirose, J.A., Vargas, C., 2005. Modelling the dynamics of the West Nile Virus. Bulletin of Mathematical Biology 67, 1157–1172.

DeBiasi, R.L., Tyler, K., 2006. West Nile Virus meningoencephalitis. Nature Clinical Practice Neurology 3 (5), 264–275.

Dohm, D.J., Sardelis, M.R., Turell, J., 2002. Experimental vertical transmission of West Nile Virus by *Culex pippiens* (Diptera: Culicidae). Journal of Medical Entomology 39 (4), 640–644.

Erni, B., Liecheti, F., Bruderer, B., 2002. Stopover strategies in passarine bird migration: a simulation study. Journal of Theoretical Biology 219, 479–493.
Fisher, R.A., 1937. The wave of advance of advantageous genes. Annals of Eugenics 7, 355–369.
FlexPDE 5.0, copyright 2005, PDE solution inc.
Goddard, L.B., Roth, A.E., Reisen, W.K., Scott, T.W., 2002. Vector competence of California mosquitoes for West Nile Virus. Emerging Infectious Diseases 8 (12), 1385–1391.
Harrington, L.C., Scott, T.W., Lerdthusnee, K., Coleman, R.C., Costero, A., Clarck, G.G., Jones, J.J., Kitthawee, S., Yapong, P.K., Sithiprasasna, R., Edman, J.D., 2005. Dispersal of the dengue vector *Aedes aegypti* within and between rural communities. American Journal of Tropical Medicine and Hygiene 72 (2), 209–220.
Hayes, G.G., 1989. West Nile virus fever. In: Monath, T.P. (Ed.), The Arboviruses Epidemiology and Ecology, vol. V. CRC Press, Florida, pp. 59–88.
Hayes, E.B., Komar, N., Nasci, R.S., Montgomery, S.P., O'Leary, D.R., Campbell, G.L., 2005. Epidemiology and transmission dynamics of West Nile Virus disease. Emerging Infectious Diseases 11 (8), 1167–1173.
Källen, A., Acuari, P., Murray, J.D., 1985. A simple model for the spatial spread and control of rabies. Journal of Theoretical Biology 116, 377–393.
Kenkre, V.M., Parmenter, R.R., Peixoto, I.D., Sadasiv, L., 2005. A theoretical framework for the analysis of the West Nile virus epidemic. Computer and Mathematics with Applications 42, 313–324.
Komar, N., Langevin, S., Hinten, S., Nemeth, N., Edwars, E., Hettler, D., Davis, B., Bowen, R., Bunning, M., 2003. Experimental infection of North American birds with the New York 1999 strain of West Nile virus. Emerging Infectious Diseases 9 (3), 311–322.
Lewis, M., Renclawowicz, J., Van den Driessche, P., 2006. Travelling waves and spread rate for a West Nile virus model. Bulletin of Mathematical Biology 68, 3–23.
Maidana, N.A., Ferreira Jr., W.C., 2008. The geographic spread of "el mal de las Caderas" in capybaras (*Hydrochaeris hydrochaeris*). Bulletin of Mathematical Biology 70 (4), 1216–1234.
Murray, J.D., Stanley, F.R.S., Brown, D.L., 1986. On the spatial spread of rabies among foxes. Proceedings of the Royal Society of London B 229, 111–150.
Murray, J.D., Seward, W.L., 1992. On the spatial spread of rabies among foxes with immunity. Journal of Theoretical Biology 156, 327–348.
Murray, J.D., 2002. Mathematical Biology. Springer, Berlin.
New York City Department of Health and Mental Hygiene, 2004. Comprehensive mosquito surveillance and control plan. ⟨http://www.nyc.gov/html/doh/downloads/pdf/wnv/wnvplan2004.pdf⟩.
Okubo, A., 1998. Diffusion-type models for avian range expansion. In: Henri Quellet, I. (Ed.), Acta XIX Congressus Internationalis Ornithologici, National Museum of Natural Sciences. University of Ottawa Press, pp. 1038–1049.
Rappole, J.H., Derrickson, S.R., Hubálek, Z., 2000. Migratory birds and spread of West Nile Virus in the western hemisphere. Emerging Infectious Diseases 6 (4), 319–328.
Reed, K.D., Meece, J.K., Henkel, J.S., Shukla, S.K., 2002. Bird migration and emerging zoonoses: West Nile virus, lyme disease, influenza A and enteropathogens. Clinical Medicine and Research 1 (1), 5–12.
Sandstede, B., 2002. Stability of traveling waves. In: Fiedler, B. (Ed.), Handbook of Dynamical System II. Elsevier, Amsterdam, pp. 983–1059.
Stewart, P.A., 1982. Migration of blue jays in eastern North America. North American Bird Bander 7 (3), 107–112.
Turell, M.J., O'Guinn, M.L., Dohm, D.J., Jones, J.W., 2001. Vector competence of North American mosquitoes (Diptera: Culicidade) for West Nile virus. Journal of Medical Entomology 38 (2), 130–134.
Volpert, A.I., Volpert, V.A., 1994. Traveling Waves Solutions of Parabolic System. American Mathematical Society, Providence, RI.
Wonham, M.J., De-camino-Beck, T., Lewis, M.A., 2004. An epidemiological model for West Nile virus: invasion analysis and control applications. Proceedings of the Royal Society of London B 271, 501–507.
Work, T.H., Hurlbut, H.S., Taylor, R.M., 1955. Indigenous wild birds of the Nile delta as potential West Nile virus circulating reservoir. American Journal of Tropical Medicine and Hygiene 4, 872–888.